Available online at www.sciencedirect.com
SCIENCE DIRECT®
Journal of the European Ceramic Society 25 (2005) 1259–1268
www.elsevier.com/locate/jeurceramsoc

Tensile strength of directionally solidified chromia-doped sapphire

J.J. Quispe-Cancapa [a,*], A.R. de Arellano-López [a], J. Martínez-Fernández [a], A. Sayir [b]

[a] *Departamento de Física de la Materia Condensada, Universidad de Sevilla, Sevilla 41071, Spain*
[b] *NASA Glenn Research Center, USA*

Available online 3 March 2005

Abstract

Tensile fracture properties of directionally solidified chromia-doped *c*-axis sapphire fibers have been studied in a range of temperature (room temperature up to 1400 °C) and dopant content (0, 300 ppm and 1% of Cr_2O_3). Delayed failure of the fibers was studied by measuring the dependence of the tensile strength on the loading rate and by fractographic studies on the fracture surfaces of the fibers. In all the temperature range, the fibers doped with 300 ppm of Cr_2O_3 are slightly stronger than the pure sapphire fibers. The least strong fibers are those containing 1% of Cr_2O_3. For this badge of material, the beneficial effect of solution hardening is counterweighted by increasing amount of defects caused by a faster fabrication. Slow crack growth appears to be the process controlling delayed failure at higher temperature. Little contribution of slow crack growth to delayed failure is found at the lower temperature.

Keywords: Sapphire; Fibres; Strength

1. Introduction

Directional solidification (DS) fabrication methods are ideal for the obtention of ceramics with special compositions and microstructures. Ceramic single-crystal and eutectic fibers is one of the significant examples.[1–8] They can be fabricated systematically, even commercially, by DS with controlled composition, allowing important fundamental studies on the physical properties of materials.

Fibers are ideal for tensile fracture studies. With a relatively simple configuration numerous fibers can be tested, addressing the intrinsic statistical behavior of fracture,[9] and a wide range of temperature can be covered.

In recent years, a systematic effort has focused on the study of the effect of dopants in fracture properties of sapphire (α-Al_2O_3), using DS fibers.[1–6,10] The addition of dopants to sapphire is known to change structural properties,[11,12] by the microscopic mechanisms of solution hardening.[13] Studies by Sayir et al.[3] showed that enhanced high temperature (HT) strength is obtained in MgO-doped sapphire, while the most efficient dopant at room temperature (RT) is Ti^{4+}. Extending a previous study by Heydt et al.,[6] that measured a clear increase in tensile strength in 100–300 ppm Cr_2O_3-doped sapphire at 1200 and 1400 °C, our work intends to complete the understanding of the effect of the addition of Cr^{3+} to the tensile fracture of α-Al_2O_3. The extension of the mentioned research follows two lines. First larger amount of dopant is used in a new badge of fibers, specially fabricated for this study. Second, the range of temperature covers from RT to 1400 °C.

There exist several approaches to the study of fracture. It is well known, for instance, that subcritical crack growth is a limitation to fracture strength in ceramics.[9,14] The stable growth of flaws under applied stresses less than that for fast fracture (slow crack growth, SCG) is experimentally studied by considering the phenomenological equation:

$$v = AK_I^N \tag{1}$$

where v is the crack velocity; K_I, stress intensity factor; and N is a constant. If N is bigger, the less likely is the material to undergo SCG.[14]

When SCG is active, both static and dynamic fatigue are important in ceramics. Static fatigue causes delayed failure and also makes the strength dependent on the rate of increase

* Corresponding author.

0955-2219/$ – see front matter © 2005 Elsevier Ltd. All rights reserved.
doi:10.1016/j.jeurceramsoc.2005.01.007

of the stress on the material. The fastest the stress is applied, the higher the strength is. Using this phenomenon, it is possible to calculate N by means of experiments in which the average strength is measured under different stressing rates.[9,14] The operant equation can be demonstrated to be:[15]

$$\sigma_f^{N+1} = B(N+1)\sigma_i^{N-2}\left(\frac{d\sigma}{dt}\right) \quad (2)$$

where σ_f is the fracture stress for a given stressing rate; σ_i, instantaneous fracture stress; and B depends on the fracture toughness, K_{Ic}, and on geometrical aspects of the critical flaw. Eq. (2) can be transformed to allow the determination of N:

$$\log(\sigma_f) = \left(\frac{1}{N+1}\right)\log\left(\frac{d\sigma}{dt}\right) + \log D \quad (3)$$

by plotting the failure stress versus the stressing rate.

2. Materials

All the materials for this study have been fabricated using directional solidification techniques. Chromia-doped sapphire (ruby) fibers were fabricated using a laser-heated floating-zone technique (LHFZ), which has been described elsewhere.[6,15] Compositions of the starting powders were 300 ppm and 10 wt.% Cr_2O_3–Al_2O_3 (sample designations NASA-L and NASA-H). Cr_2O_3 presents complete solubility in Al_2O_3,[15] however, it is well-known that chromium volatilizes at temperatures over 1000 °C,[16,17] an effect that has even been reported in certain conditions over 600 °C,[18] so actual compositions after fabrication and after the heating cycle in the mechanical testing are to be determined.

Additionally, highly-pure sapphire fibers were bought from Saphikon Inc. (Milford, NH). Saphikon fibers are fabricated by edge-defined, film fed growth technique (EFG).[19] In all cases, *c*-axis oriented crystals are used as seeds, so resulting fibers are well oriented in the *c*-axis.[4–6] Typical diameters of the fibers range from 110 to 140 μm (see Table 1 for details).

Fibers with low chromium content (NASA-L) were the subject of a previous study by Heydt et al.[6,20] Tensile rupture tests were run at both 1200 and 1400 °C, under constant strain rate. The composition of the as-fabricated and thermally cycled samples was detailed studied by secondary-ion mass-spectrometry (SIMS) and will be discussed below.

Table 1
Fiber morphological and compositional characteristics[a]

	Diameter (μm)	Temperature (°C)	Composition (Cr at.%)	
			Interior	Exterior
Saphikon	140	25–1400	0	0
NASA-L	120	25–1400	100–300 ppm	100–300 ppm
NASA-H	110	25	0.8 ± 0.2	14.5 ± 6.0
		800	0.8 ± 0.2	13.5 ± 8.5
		1200	0.9 ± 0.1	6.0 ± 5.0
		1400	1.1 ± 0.1	1.1 ± 0.1

[a] Data for NASA-L fibers are taken from Heydt.[20]

3. Experimental procedure

3.1. Mechanical tests

Mechanical experiments covered a wide range of temperature. Tensile rupture tests were performed at 25 (RT), 800, 1200, and 1400 °C. The experimental setups for 25 °C and for 1200 and 1400 °C have been described previously.[9,21,22] In the first case fibers length is 2.5 cm. In the second, 15 cm fibers are need, but the hottest zone in the $MoSi_2$ furnace is only 2.5 cm long. For experiments at 800 °C a $MoSi_2$ horizontal furnace was built and calibrated for this study. This setup uses 8 cm long fibers, and again the hottest furnace zone is 2.5 cm. Effective material volume equivalent for every condition. Experiments are only considered valid when fracture occurred in the 2.5 cm of reference, meaning less that 50% of the approximately 300 fibers that were broken in this study.

The fibers were tested under different loading rates with a device specially built and calibrated for this study. This device works by adding water to a container with a constant flow rate, ensuing a constant stressing rate. Available loading rates were 3.50×10^{-3}, 3.90×10^{-2}, 4.60×10^{-1}, and 12.60 N s^{-1}. The flow of water stops when the fiber breaks, and then the water in the container is weighted. This method allows the measurement of the tensile load of rupture with an error that can be assess to be about 1% for the slowest stressing rates and about 4.4% for the fastest, that was only used at room temperature. Typical heating and testing time is about 100 min.

3.2. Microprobe analysis and fractography

Electron microprobe analysis was conducted in a Philips XL30 scanning electron microscope equipped with secondary (SE) and backscattered (BSE) electron detectors and with a Si(Li) energy-dispersive X-ray (EDX) detector with an ultrathin window.

Semi-quantitative chemical analysis was conducted on the NASA-H samples, both as fabricated and subject to the testing thermal cycle, by EDX spectra using EDAX analytical software. Pure Al and pure Cr standards were used for quantification. Both the exterior and the interior of the fibers was analyzed. For studying sample inside, the fibers were epoxy-mounted and polished flat down to 1 μm using diamond paste. In all cases carbon was evaporated on the surfaces to make the samples conductive, with negligible effect on the spectra.

Fracture surfaces were extensively studied to identify the critical defect that originated the rupture, and also the characteristics of the crack growth. Fracture ends of the fibers were identified and saved for these fractography analysis. In the experiments run with the 15 cm fibers (higher tempera-

ture), elastic recoil after rupture was responsible for multiple fracture of the upper part of the fiber, making it impossible to identify the fracture surface. To avoid catastrophic recoil, fibers upper end was beaded[23] to hold the fiber to a syringe, that was then gripped for testing.

4. Results

4.1. Microprobe analysis

Chromium content of the different fibers are listed in Table 1. Composition of Saphikon fibers is the advertised one. The composition of NASA-L fibers was measured by Heydt et al.[6,20] NASA-H fiber composition was measured in this work.

Fig. 1 shows representative EDX composition maps for Al, Cr, and O, and an SE electron micrograph of the analyzed area for an as-fabricated NASA-H sample. Aluminum and oxygen are homogeneously distributed throughout the fiber section. Chromium, however, presents a larger concentration on the outside of the fiber, while the interior shows a lower and homogeneous concentration of the dopant.

The surface concentration of Cr in the as-fabricated samples is ∼14.5 at.%, with a large variation along the fiber. Interior Cr measurements correspond to spectral peaks well over the reference minimum detectable quantity (∼0.1%), and present a small error bar. When the fibers are cycled up to 800 °C, no significant change is found in the internal and external composition. The situation changes at 1200 °C, in good agreement with the expected volatilization of chromium over 1000 °C. On one hand the exterior of the fiber loses chromium down to half the values for lower cycle temperature, and on the other the interior gains some Cr, but the increase is still within the error bar. When cycled at 1400 °C, the composition of the interior and the exterior of the fibers balances at 1.1%. Some of the Cr evaporates, but part of it may diffuse to the inside. Again, the composition of the fiber interior appears to be homogeneous.

Fig. 2 shows additional Cr maps in sections cycled at different temperature. The corona of Cr concentration is lost at 1200 °C, as the composition of the surface an inside of the fibers balances. The lost of Cr on the surface of the sample is also evident in the optical microscopy observations, included in the figure. As-fabricated fibers present a deep red color (darker gray in the picture), that is lost as the Cr of the surface volatilizes. All these features do not mean any change in the fiber morphology or diameter, as seen in the SE micrographs in Fig. 2.

As a general result, the interior of the NASA-H fibers contains ∼1 at.% of chromium for all the temperature interval. Effectively the range of fiber compositions then covers 0 Cr% (Saphikon), ∼300 Cr ppm (NASA-L), and ∼1 Cr% (NASA-H).

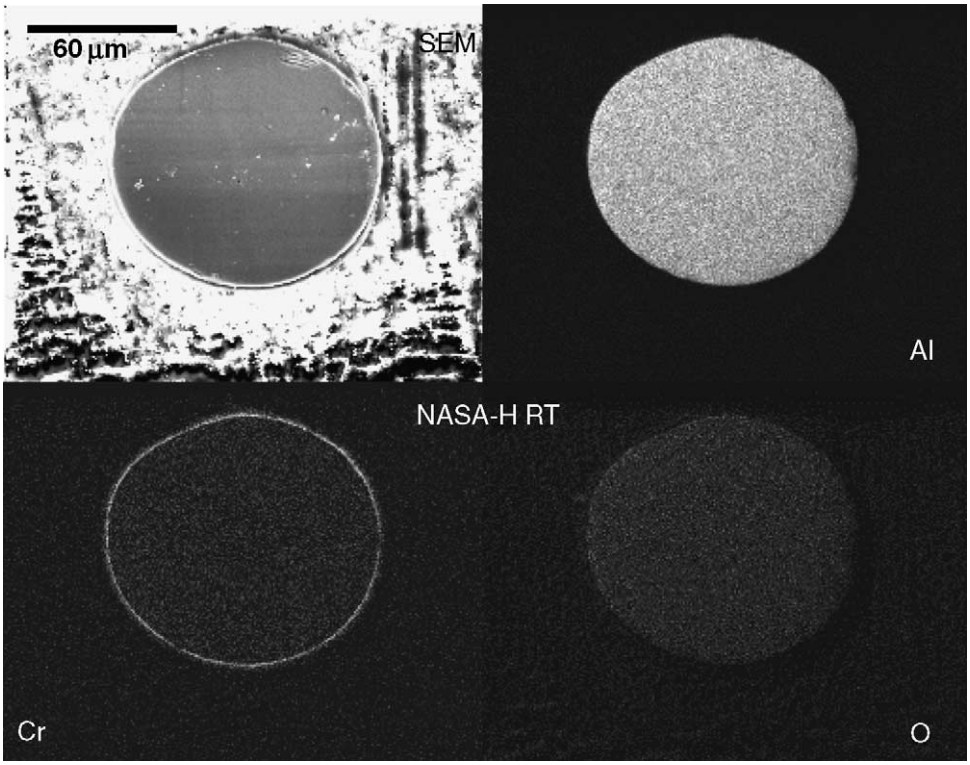

Fig. 1. Energy-dispersive X-ray maps, for aluminum, chromium and oxygen, and corresponding secondary electron SEM micrograph of an as-fabricated NASA-H fiber. The accumulation of Cr on the exterior of the fiber is evident.

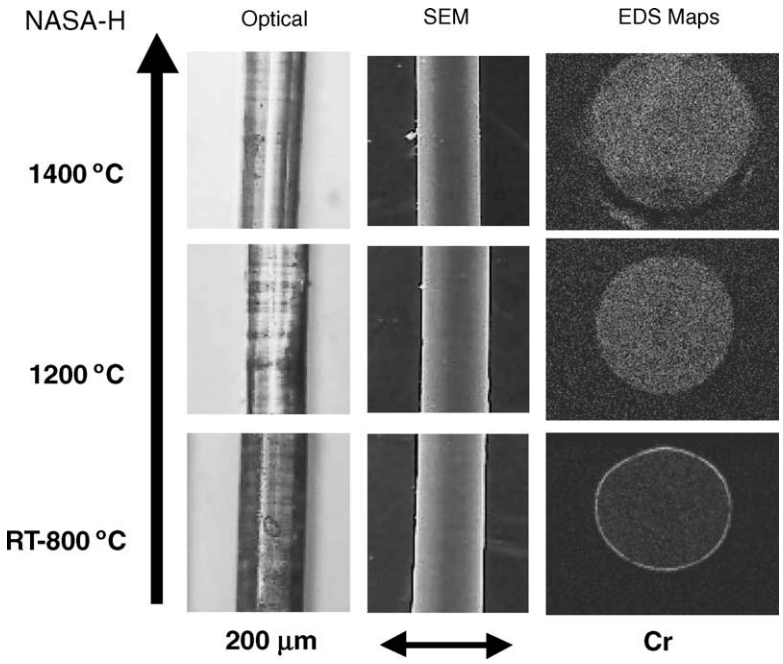

Fig. 2. Optical microscopy, SEM, and EDS mapping micrographs of NASA-H fibers cycled up to 800, 1200, and 1400 °C. The morphology of the fiber is unchanged, but the volatilization of Cr is evident for 1200- and 1400 °C-cycled fibers, both by the loose of deep-red color of the fibers (grey in the micrographs), and the absence of the Cr corona in the exterior of the fibers as seen in the EDS maps.

4.2. Mechanical tests

In mechanical experiments rupture stress, σ_f, is measured for different stressing rates, $\dot{\sigma}$. Rupture stress versus stressing rate plots from our study, for different temperature and type of fibers are shown in Figs. 3–6, and the average values are listed in Table 2, along with corresponding error bars. The listed results for NASA-L fibers at 1200 and 1400 °C are taken from the previous work by Heydt et al.,[6,20] that tested the fibers using a constant strain rate apparatus, and calculated the stressing rate assuming elastic conditions.

Fracture is an statistical phenomenon, that is dominated by the presence of critical defects,[6] so it is typical to find large scatter in the rupture stress. Even under this consideration, several trends are evident. The tensile strength decreases systematically with temperature for every type of fiber. NASA-L fibers are the strongest ones at every temperature, but results are within the experimental error when compared to the Saphikon fibers. NASA-H fibers, with the largest Cr content, are the weakest, with a lost of strength near to 50% when compared to NASA-L fibers.

Additionally, an increase of the average tensile strength with stressing rate is evident, at every temperature. This means that a value of N can be calculated according to Eq. (3). When this value is large (>40), then the slope of the σ_f versus $\dot{\sigma}$ curve is very flat, so more experiments are need for a better determination of N, with a wider interval of stressing rates, as seen in the table (10^{-1} to 10^{3} MPa s^{-1}, in orders of magnitude). Such is the case for the room temperature results (Fig. 3). At this temperature more experiments are possible because the testing technique uses smaller fibers.

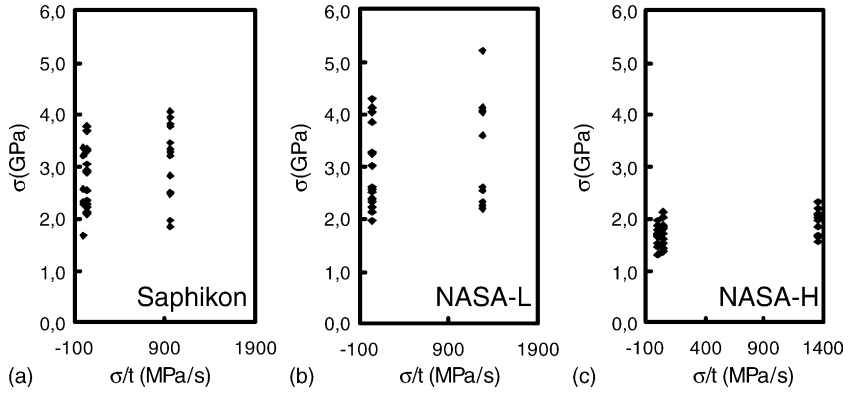

Fig. 3. Room-temperature tensile rupture results for: (a) Saphikon, (b) NASA-L, and (c) NASA-H fibers.

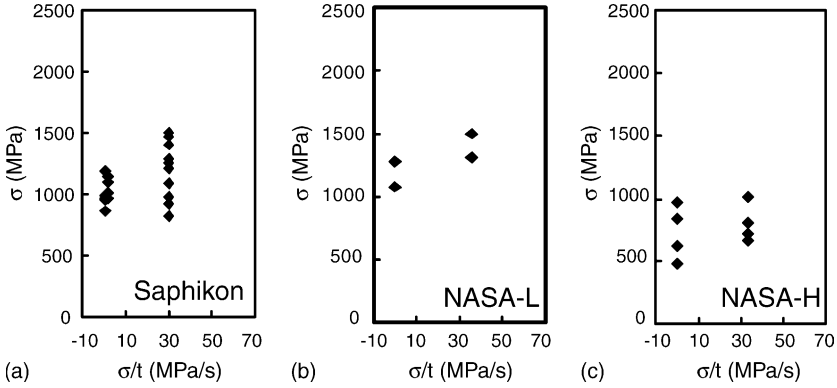

Fig. 4. 800 °C tensile rupture results for: (a) Saphikon, (b) NASA-L, and (c) NASA-H fibers.

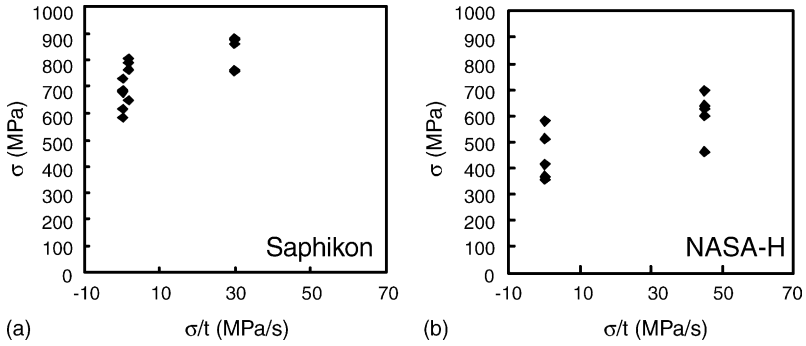

Fig. 5. 1200 °C tensile rupture results for: (a) Saphikon and (b) NASA-H fibers.

As a general scope, N is larger at room temperature and 800 °C than at 1200 and 1400 °C. The N values are determined by linear regression when three data points are available. In all cases $R^2 > 0.90$.

4.3. Fractography

Representative fracture surfaces of the fibers are shown in the micrographs of Figs. 7–10, for fibers broken at room temperature, 800, 1200, and 1400 °C, under different stressing rates. In all cases fracture origin is a fiber defect, either internal or external. No difference on fracture surface features has been found to be correlated to stressing rate.

The qualitative features of fracture surfaces are typical, and are a result of changes in the crack growth velocity.[9,24] Micrographs in Figs. 9 and 10, corresponding to the higher temperature experiments, present all the significant characteristics: the fracture source is easily identified, and it is surrounded by a small region that is considered to be originated by the slow crack growth.[4,24,25] Micrographs in Fig. 11 show details of this type of feature generally found in NASA-H fibers broken at 1200 and 1400 °C. Around it, a smooth mirror region is clearly seen. When the crack front is large enough, when high crack velocity has been reached, crack branching is evident,[24,25] probably following sapphire crystallographic planes.[26]

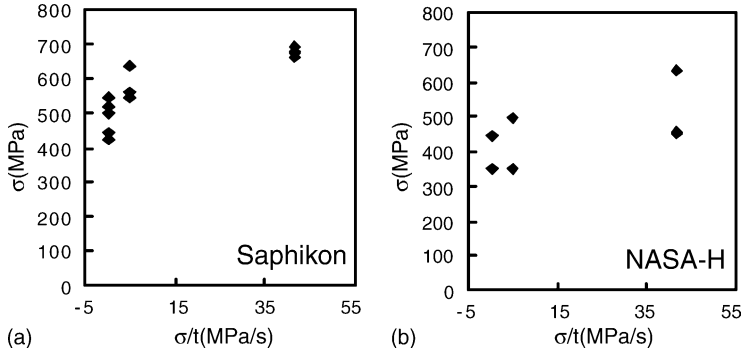

Fig. 6. 1400 °C tensile rupture results for: (a) Saphikon and (b) NASA-H fibers.

Table 2
Comprehensive summary of mechanical results[a]

Fibers	25 °C				800 °C				1200 °C				1400 °C			
	$\dot{\sigma}$ (MPa s^{-1})	σ_f (MPa)	$\Delta\sigma_f$ (MPa)	N	$\dot{\sigma}$ (MPa s^{-1})	σ_f (MPa)	$\Delta\sigma_f$ (MPa)	N	$\dot{\sigma}$ (MPa s^{-1})	σ_f (MPa)	$\Delta\sigma_f$ (MPa)	N	$\dot{\sigma}$ (MPa s^{-1})	σ_f (MPa)	$\Delta\sigma_f$ (MPa)	N
Saphikon	0.38	2572	630	44	0.3	987	119	24	0.3	659	58	19	0.37	487	51	13
	35	2884	624		1.8	1050	79		1.8	752	70		5.0	582		
	950	3061	735		29.9	1189	236		29.9	836	60		41.5	675		
NASA-L	0.47	2683	650	45	0.2	1177	144	28	0.37	815	380	11	0.37	736	444	14
	48	2966	788		35	1406	129		39	1190	395		39	969	332	
	1274	3189	630						4236	1735	490		4236	1400	213	
NASA-H	0.52	167	198	54	0.31	730	221	50	0.28	447	95	16	0.5	397	67	19
	44	1731	248		33	800	152		45	604	86		5.0	455	110	
	1353	1938	253										41.5	515	103	

[a] Results for NASA-L fibers at 1200 and 1400 °C are taken from Heydt.[20]

As the testing temperature decreases, the slow crack growth region disappears and the mirror region is smaller. This observation is clear in the micrographs in Figs. 6 and 7. In Saphikon fibers broken at room temperature, the mirror region is absent.

5. Discussion

Some studies on strength of pure are doped sapphire are now classical.[11,12,27] The tensile strength results of sapphire-based fibers, with different dopants and compositions, are presented in Fig. 12. The results of this study, plotted for comparison in this graph, correspond to the fracture stress in the experiments using the slowest stressing rates, that are the lowest at each temperature, as presented in Table 2. The results from other studies[3–5] correspond to different stressing rate conditions, not always specified. It is to be beard in mind, however, that even large changes in the stressing rates only cause small changes in average tensile strength, so qualitative comparison is possible.

The general trend of our results is parallel to that of other works, in terms of the reduction of strength with temperature. Results on Saphikon fibers is similar in the different studies at RT and at the highest temperature, but not in the intermediate range. At 800 °C, for instance, Newcomb and Tressler,[4] report a tensile strength higher than that reported by Sayir,[5] and twice the value measured in this study. It will be shown below, that it is also in the range RT to 800 °C where larger differences in the exponent N are found between different studies.

For similar dopant content of a few hundred parts per million, it is apparent that Cr is less effective than Mg and Ti as additive for improving strength. Sapphire doped with cations with ionic radius larger than Al^{3+} is expected to be stronger than pure sapphire due to the mechanism of solution hardening.[13,28] Larger ions cause a deformation of the network, and make the sliding of dislocations more difficult. An increasing size of the cations produce a larger deformation of the network, and eventually increasing strengths. Considering Mg, Ti and Cr, the expected result is: $\sigma_{Mg^{2+}} > \sigma_{Ti^{4+}} > \sigma_{Cr^{3+}}$ [11] which is the measured result at HT.

The classical model of solution hardening by a small concentration of discrete obstacles[28] establishes that the improved yield strength, σ, is:

$$\sigma \propto f^{3/2} c^{1/2} \tag{4}$$

where f is related to the energy barrier of each obstacle, then related to the cation size, and c is the dopant concentration. For small additions of dopant, the main effect on strength is related to the energy barrier to dislocation sliding imposed the solute.

Considering Eq. (4), increasing dopant concentration should result in bigger yield stress. This is not our obser-

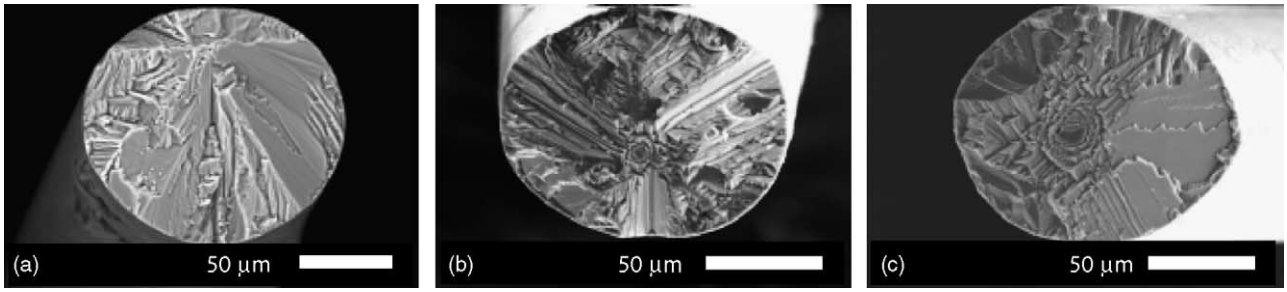

Fig. 7. SEM micrographs of fracture surfaces of: (a) Saphikon, (b) NASA-L, and (c) NASA-H fibers fractured at room-temperature.

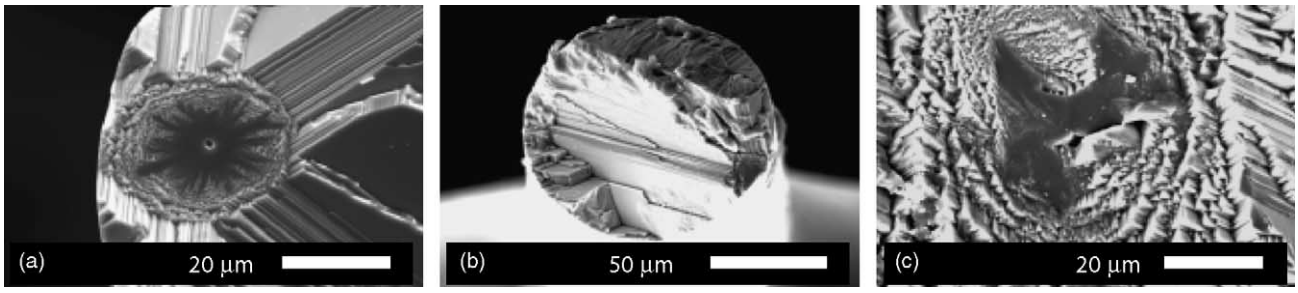

Fig. 8. SEM micrographs of fracture surfaces of: (a) Saphikon, (b) NASA-L, and (c) NASA-H fibers fractured at 800 °C.

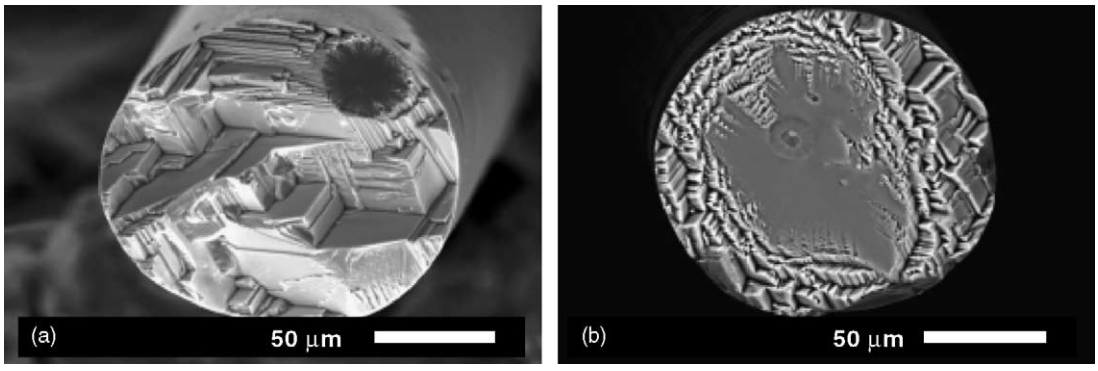

Fig. 9. SEM micrographs of fracture surfaces of: (a) Saphikon and (b) NASA-H fibers fractured at 1200 °C.

vation, however. The addition of larger amounts of Cr, up to 1 at.%, reduces strength in all the temperature range. Most likely explanation is the possibility of being the NASA-H fibers more imperfect than other formulations. To achieve larger Cr contents in the fibers, a more rapid laser-heating cycle is needed, which probably results in more internal cavities. This type of defects are always the origin of fracture in NASA-H fibers in the whole range of temperature. In

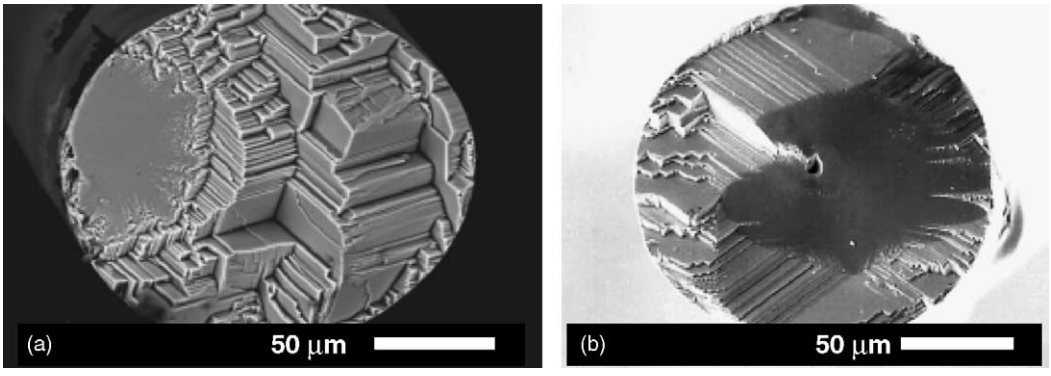

Fig. 10. SEM micrographs of fracture surfaces of: (a) Saphikon and (b) NASA-H fibers fractured at 1400 °C.

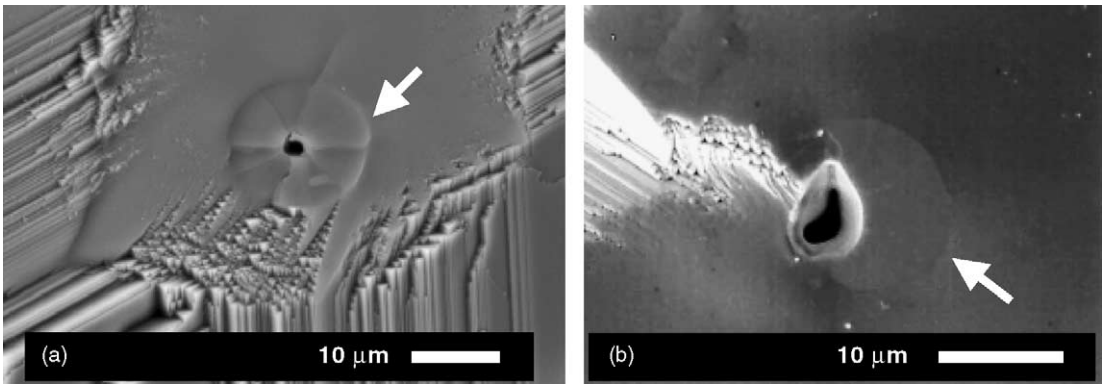

Fig. 11. SEM micrographs showing details of crack growth around the critical defects in NASA-H fibers fractured at: (a) 1200 °C and (b) 1400 °C.

Saphikon and NASA-L fibers both internal and external defects are detected to be fracture origin.

Previous studies[21,22] reported that RT Weibull modulus is about 4 for Saphikon and NASA-L and about 8 for NASA-H fibers, which would support the suggestion of a larger defect population in the NASA-H fibers. The evolution of Weibull modulus with temperature (800–1400 °C range) in Saphikon fibers was studied by Sayir. He found an increase in the modulus from about 5 to about 18, with increasing temperature, and correlated the effect with a growing activity of SCG with temperature.[5]

In the plots of Fig. 13, the results listed in Table 2 are compared with literature results. When these literature results are from constant strain rate experiments, the transformation to constant stressing rate is made assuming a elastic behavior, with a representative $E_{[0\,0\,0\,1]}$ = 335 GPa. The dependence of this value with temperature is weak.[9] The results on the NASA-L fibers at 1200 and 1400 °C are taken from the work of Heydt et al.[6] Previous assertions on strength, now under different stressing rates, hold. A dependence of strength on stressing rate has been measured at every temperature, suggesting that static fatigue may be active. Such result, however, is indisputable only as temperature increases.

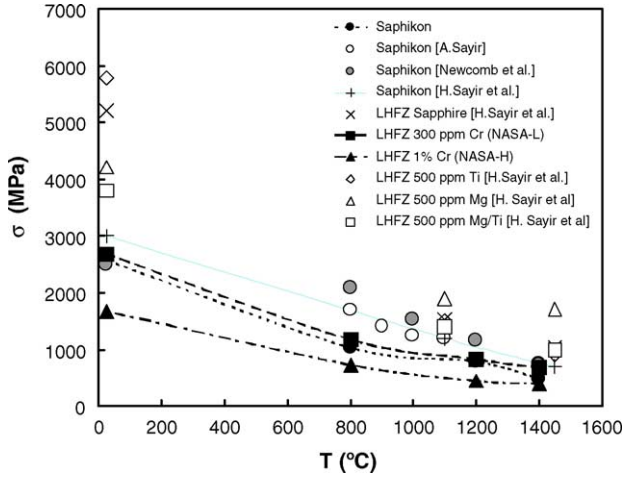

Fig. 12. Tensile strength results vs. temperature from this study for the slowest stressing rate (0.2–0.5 MPa s^{-1}), compared to literature results from Sayir et al.,[3] Newcomb and Tressler[4] and Sayir.[5]

All the plots in Fig. 13 used the same scale in the axis, so the slopes are directly comparable. These slopes are more flat at RT than at 1200 or 1400 °C, meaning a decrease in the value of N with temperature. In Fig. 14, the N values calculated in this study are plot versus temperature, including some literature results.[4,5] Two regions are clearly distinguishable. From RT up to 1000 °C, N is larger than 20. Results by different authors present a significant scatter, but N as high as 54 has been calculated in our study for NASA-H at RT. From 1100 up to 1500 °C, the interval for N is in the range 10–20.

When combine with the fractographic observations, it is possible to suggest that SCG plays a role in the HT tensile strength of Cr-doped sapphire fibers, then explaining the observed dependence of the strength on the stressing rate. At lower temperature, N values are high, meaning a weak dependence of the strength on the stressing rate, and fracture surfaces do not present evidence of SCG. Static fatigue by SCG is then basically a HT phenomenon is DS sapphire-based fibers, confirming observations by several authors.[3–6,12]

Several microscopic mechanisms have been claimed responsible for the SCG process, from which we consider four: stress corrosion,[29] diffusive cavitation,[30] dislocation assisted crack growth[31] and thermally activated bond rupture.[32] Microstructural observations that may support the activity of these mechanisms are quite difficult, when not impossible for the characteristics of the samples, fibers in this case, so speculation may only rule out a mechanisms tentatively.

In the range of temperature for which SCG is active, the HT range, fracture origin is typically an internal defect, with some exceptions in some experiments on Saphikon fibers at 1400 °C, so stress corrosion is unlikely to be the SCG mechanism. Pore diffusive-growth in crack-like manner is also quite unlikely in sapphire, given the shortness of the experiment, and the slow diffusivities of atomic species in Al_2O_3. More detailed arguments can be found in the literature.[4] Dislocation-assisted mechanisms can be also ruled out. Given the orientation of the fibers, and the experimental conditions, if plastic deformation was important at the crack tips twinning

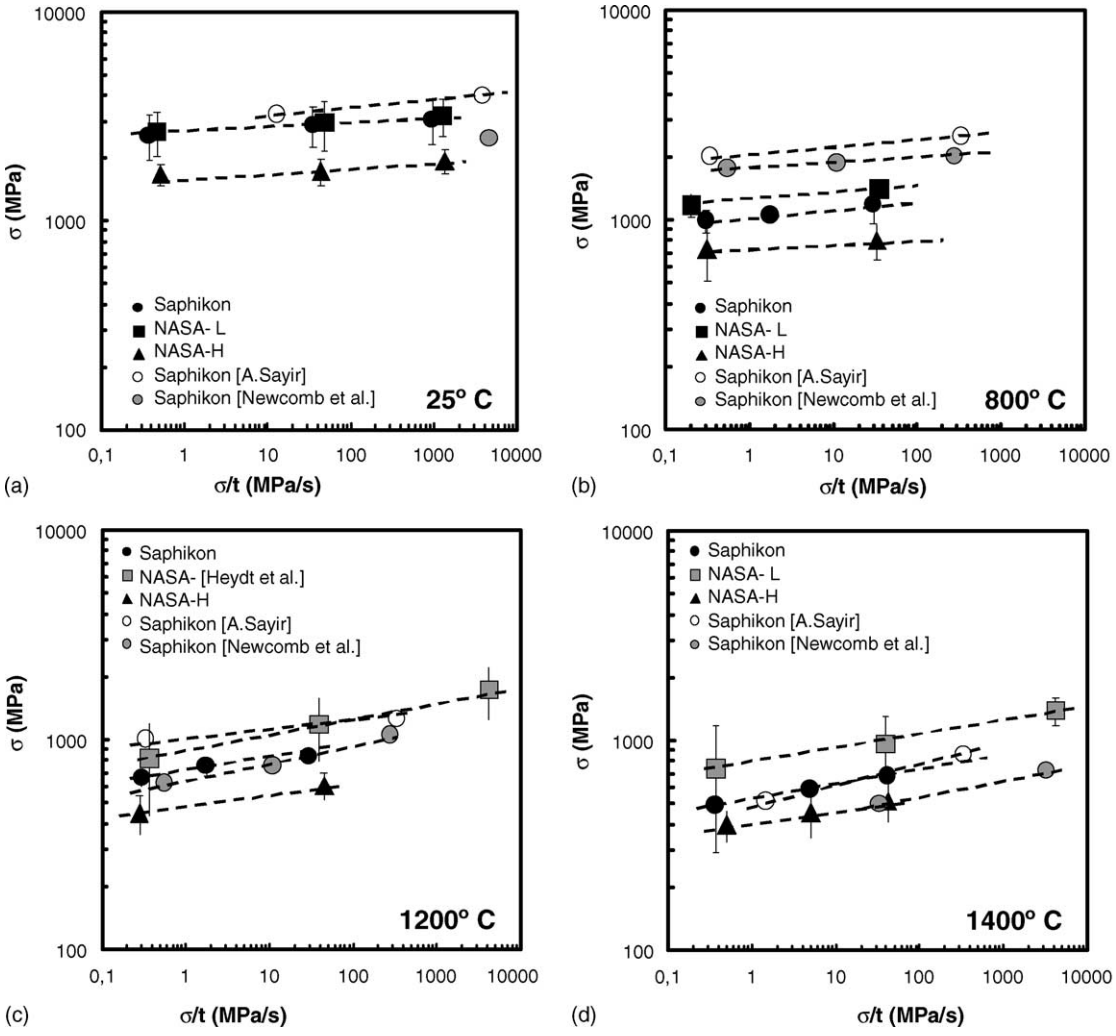

Fig. 13. Tensile strength results vs. stressing rate for different temperatures (a) 25 °C, RT, (b) 800 °C, (c) 1200 °C, and (d) 1400 °C. Some literature results from Heydt et al.,[6] Newcomb and Tressler[4] and Sayir[5] are also included for comparison.

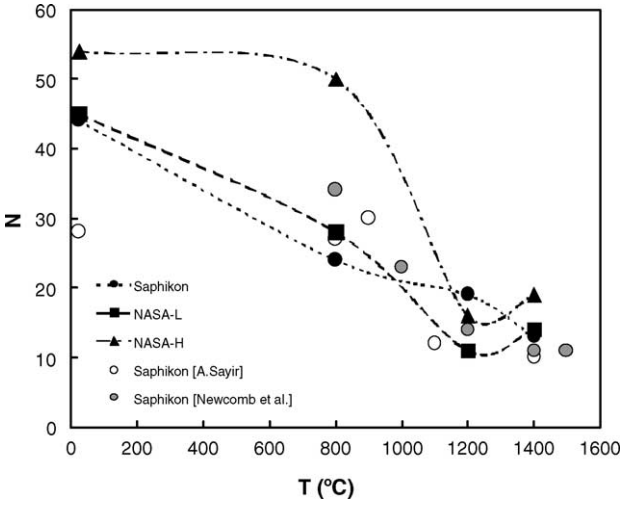

Fig. 14. Values of the exponent *N* for different temperature. Results from Newcomb and Tressler[4] and Sayir[5] are also included for comparison.

should be observed.[33] Mirror surfaces are flat and smooth and no striations are observed in the exterior of the fibers.

The most plausible SCG mechanism is thermally activated bond rupture. Newcomb and Tressler[4] suggest the mechanisms of lattice trapping[32] for HT-SCG in Saphikon fibers, and provide several qualitative supporting features, both mechanical and microstructural. Among the last, the topography of the fracture surfaces is of most importance. The particular shape of the branching along crystallographic planes, which is dominated by the differences in crack propagation velocity through those planes, is predicted by the lattice trapping mechanisms.

6. Conclusions

Directionally solidified pure sapphire and chromia-doped sapphire *c*-axis fibers, have been studied in tension from room temperature to high temperature under a range of stressing rates. NASA-L fibers are stronger than Saphikon fibers, and

both stronger than NASA-H fibers. Solution hardening is suggested to be responsible for the increase of tensile strength in the fibers with low dopant content, and internal defects are considered responsible of the reduction of tensile strength in the fibers with high dopant content. High-temperature static fatigue is found in all the fibers. Slow crack growth is the dominant process to explain the dependence of the tensile strength on the stressing rate. Thermally activated bond rupture is suggested to be the microscopic mechanism controlling HT-SCG in these sapphire-based fibers.

Acknowledgment

This research was funded at NASA by AFOSR Grant #F49620-00-1-0048, NASA NCC3-850 and in Spain by MCyT grant MAT2000-1533-C03-03.

References

1. Haggerty, S., Growth of titanium and chromium strengthened sapphire fibers. *Technical Report AFML-TR-73-2*. Air Force Materials Laboratory, WPAFB, OH, 1972.
2. Crane, R. L., An investigation of the mechanical properties of silicon carbide and sapphire filaments. *Technical Report AFML-TR-72-180*. Air Force Materials Laboratory, WPAFB, OH, 1972.
3. Sayir, H., Farmer, S. C., Lagerlof, K. P. D. and Sayir, A., Temperature dependent fracture strength of doped single-crystal alumina fibers. In *Advances in Ceramic-Matrix Composites II*, ed. J. P. Singh and N. P. Bansal, pp. 53–63. *Ceramic Transactions, Vol 46*. The American Ceramic Society, Westerville, OH, 1994.
4. Newcomb, S. A. and Tressler, R. E., Slow crack growth in sapphire fibers at 800° to 1500 °C. *J. Am. Ceram. Soc.*, 1993, **76**(10), 2505–2512.
5. Sayir, A., Time dependent strength of sapphire fibers at high temperatures. In *Advanced Ceramic-Matrix Composites*, ed. N. P. Bansal, pp. 691–703. *Ceramic Transactions, Vol 38*. The American Ceramic Society, Westerville, OH, 1993.
6. Heydt, P. E., Tressler, R. E. and Sayir, A., Delayed failure of Cr^{3+}-doped sapphire fibers. In *Advances in Ceramic-Matrix Composites III*, ed. N. P. Bansal and J. P. Singh, pp. 67–75. *Ceramic Transactions, Vol 74*. The American Ceramic Society, Westerville, OH, 1996.
7. McClellan, K. J., Sayir, H., Heuer, A. H., Sayir, A., Haggerty, J. S. and Sigalovsky, J., High-temperature creep-resistant Y_2O_3-stabilized cubic ZrO_2 single-crystal fibers. In *Advances in Ceramic-Matrix Composites II*, ed. J. P. Singh and N. P. Bansal, pp. 63–73. *Ceramic Transactions, Vol 46*. The American Ceramic Society, Westerville, OH, 1994.
8. Martinez-Fernández, J., Sayir, A. and Farmer, S. C., High-temperature creep deformation of directionally solidified $Al_2O_3/Er_3Al_5O_{12}$. *Acta Mater.*, 2003, **51**, 1705–1720.
9. Wachtman, J. B., *Mechanical Properties of Ceramics*. Wiley, 1996.
10. Quispe Cancapa, J. J., de Arellano Lopez, A. R. and Sayir, A., High-temperature mechanical properties of directionally solidify Cr^{3+} sapphire fibers. *Ceram. Eng. Sci. Proc.*, 2002, **23**(3), 665–673.
11. Radford, K. C. and Pratt, P. L., The mechanical properties of impurity-doped alumina single crystal. *Br. Ceram. Soc.*, 1970, **15**, 185–202.
12. Pletka, M. L., Mitchell, T. E. and Heuer, A. H., Strengthening mechanisms in sapphire. In *Fracture Mechanics of Ceramics* (*Vol 2*), ed. R. Bradt *et al.* Plenum Press, New York, 1974, pp. 181–194.
13. Butt, M. Z. and Feltham, P., Review of solid-solution hardening. *J. Mater. Sci*, 1993, **28**, 2557.
14. Barsoum, M. W., *Fundamentals of Ceramics*. McGraw-Hill, 1997.
15. Westfall, L., Sayir, A. and Penn, W., System grows single-srystal fiber. *NASA Tech. Briefs*, 1994, **18**(8), 77.
16. Bunting, E. N., Phase diagrams Al_2O_3–Cr_2O_3. *Bureau Standards J. Res.*, 1931, **6**(6), 948.
17. *CRC Handbook of Materials Science* (*Vol I*), ed. C. T. Lynch. CRC Press, 1986.
18. Asteman, H., Svensson, J. E., Johansson, L. G. and Norell, M., Indication of chromium-oxide hydroxide evaporation during oxidation of 304 L at 873 K in the presence of 10-percent water-vapor. *Oxidat. Met.*, 1999, **52**(1/2), 95–111.
19. LeBelle, H. E., Growth of controlled profile crystals from the melt. Part II: Edge-defined, film-fed growth. *Mater. Res. Bull.*, 1971, **6**, 581–590.
20. Heydt, P. E., Master Thesis. Pennsylvania State University, 1996.
21. Quispe Cancapa, J. J., de Arellano Lopez, A. R. and Sayir, A., Room- and high-temperature tensile fracture of directionally solidified chromia-doped sapphire fibers. *Ceram. Eng. Sci. Proc.*, 2003, **24**, 135–142.
22. Quispe Cancapa, J. J., Master Thesis. Universidad de Sevilla, 2002.
23. Kotchick, D. M., Ph.D. Thesis, Pennsylvania State University, 1978.
24. Rice, R. W, *Fractography of Glasses and Ceramics*, ed. J. R. Varner and V. D. Frechette. *Adv. Ceram.*, 1986, **22**, 3–56.
25. Rice, R. W. and Becher, P. F., Comment of creep deformation of 0° sapphire. *J. Am. Ceram. Soc.*, 1977, **60**(3/4), 186–188.
26. Kirchner, H. P., Brittleness dependence of crack branching in ceramics. *J. Am. Ceram. Soc.*, 1986, **89**(4), 339–342.
27. Firestone, R. F. and Heuer, A. H., Creep deformation of 0° sapphire. *J. Am. Ceram. Soc.*, 1976, **59**(1/2), 24–29.
28. Chandrasekaran, D., Solution hardening—a comparison of two models. *Mater. Sci. Eng.*, 2001, **A309/A310**, 184–189.
29. Wiederhorn, S. E., *Fracture Mechanics of Ceramics* (*Vol 2*), ed. R. Bradt *et al*. Plenum Press, New York, 1974, pp. 613–646.
30. Chuang, T., A diffusive crack-growth model for creep fracture. *J. Am. Ceram. Soc.*, 1982, **65**(2), 93–103.
31. Lawn, B. R., Physics of fracture. *J. Am. Ceram. Soc.*, 1983, **66**(2), 83–91.
32. Thomson, R., Hsieh, C. and Rana, V., Lattice trapping of fracture cracks. *J. Appl. Phys.*, 1971, **42**, 3154–3160.
33. Castaing, J., Muñoz, A., Gome Garcia, D. and Dominguez Rodriguez, A., Basal slip in sapphire (α-Al_2O_3). *Mater. Sci. Eng.*, 1997, **A233**, 121–125.